Macromolecules
ARTICLE

Macromolecules **2010**, *43*, 8531–8538 **8531**
DOI: 10.1021/ma101677t

High Surface Area Networks from Tetrahedral Monomers: Metal-Catalyzed Coupling, Thermal Polymerization, and "Click" Chemistry

James R. Holst, Ev Stöckel, Dave J. Adams, and Andrew I. Cooper*

Department of Chemistry and Centre for Materials Discovery, University of Liverpool, Crown Street, Liverpool L69 7ZD, United Kingdom

Received July 26, 2010; Revised Manuscript Received September 12, 2010

ABSTRACT: A series of tetrahedrally linked conjugated microporous polymer networks were prepared using a variety of bond-forming chemistries including Sonogashira−Hagihara coupling, Yamamoto coupling, thermal alkyne condensation, and "click" chemistry. These thermally stable polymers exhibit high surface areas (up to 3200 m^2/g) and adsorb up to 2.34 wt % hydrogen by mass at 1.13 bar/77 K and 7.59 wt % carbon dioxide by mass at 1.13 bar/298 K.

Introduction

The design and synthesis of microporous organic polymers has attracted significant interest due to their potential application in the areas of molecular separations, heterogeneous catalysis, and gas storage.[1−4] A number of different classes of microporous organic networks have been reported. Covalent organic frameworks (COFs)[5−7] are crystalline organic networks which are analogous to metal−organic frameworks (MOFs). COFs have achieved some of the highest surface areas among organic materials (up to 4210 m^2/g), but physicochemical stability for boron-linked COFs is a potential concern. Crystalline imine-linked COF variants have been developed which address this stability issue.[7] Robust covalent triazine frameworks (CTFs) have also been synthesized in molten $ZnCl_2$ at temperatures in excess of 400 °C, and these materials have achieved Brunauer−Emmett−Teller (BET) surface areas (SA_{BET}) approaching 3000 m^2/g.[8,9] Hyper-cross-linked polymers (HCPs)[10−13] can be prepared via Friedel−Crafts routes, generating surface areas up to 2090 m^2/g,[11] although the scope for synthetic diversification by such routes is perhaps limited. Polymers of intrinsic microporosity (PIMs)[14] utilize highly contorted monomers to produce both insoluble networks and linear, soluble polymers which demonstrate surface areas up to 1790 and 750 m^2/g, respectively.[15−18]

In 2007, our research group reported the synthesis of conjugated microporous polymers (CMPs) via Sonogashira−Hagihara cross-coupling chemistry.[19] Palladium-catalyzed cross-coupling of aromatic halides with aromatic ethynyl compounds led to porous poly(aryleneethynylene) (PAE) networks[20−22] with BET surface areas in excess of 1000 m^2/g in some cases. We also found that the size of the pores within the structure could be controlled by tuning the strut length between the linking monomers.[21] In particular, we showed that shorter strut lengths produced larger surface areas. Subsequently, our research group and others have reported a range of synthetic strategies to produce CMP networks.[23] These synthetic methods include the Gilch reaction,[24] alkyne−alkyne homocoupling,[25] Suzuki coupling,[26,27] thienyl coupling via oxidative polymerization,[4,28] chemical trimerization of aromatic alkynes,[29,30] aldol condensation,[31] and Yamamoto polymerization.[32,33]

*Corresponding author. E-mail: aicooper@liverpool.ac.uk.

Recently, the Yamamoto polymerization of a tetrahedral-based monomer produced a rigid network (PAF-1) with an unprecedented BET surface area of 5640 m^2/g.[33] This is the highest surface area reported for a purely organic porous material, and the value approaches the largest surface area exhibited in a MOF (MOF-210; 6240 m^2/g).[34] PAF-1 also combines exceptional surface area with impressive physicochemical stability.[33] For example, its porosity is unchanged by boiling in water for 1 week. Purely tetrahedral networks have been reported before. One example is the imine-linked network COF-300, mentioned above.[7] Also, Kaskel and co-workers reported the synthesis of microporous hydrophobic polysilanes via an organolithiation route (SA_{BET} up to 1046 m^2/g).[35] We too described the synthesis of carbon- and silicon-centered tetrahedral CMP networks, and these materials showed some of the highest surface areas among the materials that we have synthesized via Sonogashira−Hagihara coupling chemistry (SA_{BET} = 1213 m^2/g).[36]

PAF-1 confirms in spectacular fashion the benefit of three-dimensional tetrahedral monomers in terms of obtaining high surface areas. As yet, there are few systematic explorations of the range of chemistry than can be deployed to produced such tetrahedral networks. We describe here a series of CMP networks based on tetrahedral monomers with surface areas that range from 1100 to 3200 m^2/g. In particular, we show that a variety of synthetic routes (cross-coupling, homocoupling, thermal alkyne condensation, and "click" chemistry) are possible and that all routes give rise to robust microporous networks.

Experimental Section

Materials. Bis(1,5-cyclooctadiene)nickel(0) and tetrakis(triphenylphosphine)palladium(0) were obtained from Alfa Aesar and used as received. Tetrakis(4-aminophenyl)methane was purchased from Manchester Organics in 98% purity. All other chemicals and solvents were obtained from Sigma-Aldrich and used as received. Anhydrous grade solvents were used throughout (Sigma-Aldrich). All chemicals used had a purity of 97% or greater. Tetrakis(4-iodophenyl)methane[37] (TIPM), tetrakis(4-bromophenyl)adamantane[38] (TBPA), tetrakis(4-bromophenyl)-silane[39] (TBPS), and tetrakis(4-ethynylphenyl)methane[29] (TEPM) were synthesized according to previously reported literature.

Synthesis of Tetrakis(4-azidophenyl)methane. This reaction was slightly modified from the previous report.[40] Tetrakis(4-aminophenyl)methane (500 mg, 1.31 mmol) was added to 10 mL

Published on Web 09/28/2010

of H_2O, then 5 mL of concentrated HBF_4 was added to dissolve the suspension. The mixture was cooled to −10 °C in a salt−ice bath. A solution of sodium nitrite (543 mg, 7.87 mmol) in H_2O (3 mL) was slowly added to the acid solution. An aqueous solution (3 mL) of sodium azide (433 mg, 6.66 mmol) was slowly added dropwise to the intermediate diazonium salt. (**Safety note**: *Sodium azide is highly toxic and potentially explosive. Furthermore, the evolution of hydrazoic acid (HN_3) is possible under acidic conditions. All manipulations should be carried out in a fume cupboard and behind a blast shield.*) The mixture was stirred overnight. The precipitate was filtered off and washed with copious water. The gray solid was dissolved in chloroform and filtered through Celite. The filtrate was slowly evaporated to collect light brown crystals, which were dried in air. Yield: 68%. ^{1}H NMR ($CDCl_3$, 400 MHz): 7.14 (d; 8H; Ar−*H*), 6.94 (d; 8H; Ar−*H*) ppm. ^{13}C NMR ($CDCl_3$, 100 MHz): δ 142.87, 138.17, 132.07, 118.43, 63.23 ppm.

Synthesis of Networks 1−3. In a typical procedure, bis(1,5-cyclooctadiene)nickel(0) (2.25 g, 8.18 mmol, Alfa Aesar) and 2,2′-bipyridyl (1.28 g, 8.18 mmol) were added to a flame-dried round bottomed flask in a glovebag under inert conditions. The sealed flask was removed from the glovebag, and anhydrous DMF (~120 mL) was transferred to the flask via a double-ended needle. 1,5-Cyclooctadiene (1.05 mL, 8.32 mmol) was added to the solution and stirred for 1 h at 80 °C. To the resulting purple solution, the tetrahalogen monomer (1.57 mmol) was added. The solution was stirred at 80 °C for 24 h. After cooling to room temperature, the reaction mixture was quenched with concentrated HCl (~50 mL). The reaction mixture was stirred overnight, ensuring that the solution had turned green. The floating precipitate was collected by filteration and washed with $CHCl_3$ (150 mL), THF (150 mL), and H_2O (150 mL), ensuring that the distinct smell of cyclooctadiene was not present anymore. The resulting material was then Soxhlet extracted in a suitable solvent to remove all remaining monomer. Yields for **1**, **2**, and **3**: 87%, 60%, and 134%, respectively, based on hypothetical 100% polycondensation.

Synthesis of CMP Network 4. In a typical procedure, tetrakis-(4-iodophenyl)methane (200 mg, 0.24 mmol), tetrakis(4-ethynylphenyl)methane (150 mg, 0.36 mmol), tetrakis(triphenylphosphine)palladium(0) (20 mg, 7 mol %), and copper iodide (6 mg, 14 mol %) were added to a oven-dried 100 mL Radleys flask and condenser. The apparatus was evacuated under reduced pressure and backfilled with N_2 five times. Anhydrous DMF (10 mL) was added via syringe, followed by (10 mL) anhydrous diisopropylamine. The reaction mixture was heated at 80 °C for 24 h. Once cooled to room temperature, the resultant polymer was filtered off and washed with chloroform, tetrahydrofuran, methanol, and acetone. Three consecutive Soxhlet extractions were performed overnight with methanol, THF, and $CHCl_3$. The product was then dried in a vacuum oven at 60 °C for 24 h. Yield: 154% based on hypothetical 100% polycondensation.

Synthesis of Homocoupled Network 5. Tetrakis(4-ethynylphenyl)-methane (150 mg, 0.36 mmol), dichlorobis(triphenylphosphino)-palladium(II) (10 mg, 4 mol %), triphenylphosphine (11 mg, 12 mol %), and copper iodide (3 mg, 4 mol %) were added to a oven-dried 100 mL Radleys flask and condenser. The apparatus was evacuated under reduced pressure and backfilled with N_2 five times. Anhydrous DMF (15 mL) and diisopropylamine (5 mL) were added via syringe. The reaction mixture was heated at 70 °C for 86 h. Once cooled to room temperature, the product was filtered off and washed with THF, methanol, and acetone. The product was further washed by Soxhlet extraction in methanol for 18 h. Yield: 99% based on hypothetical 100% polycondensation.

Synthesis of Thermally Polymerized TEPM Network 6. Tetrakis-(4-ethynylphenyl)methane (71 mg, 0.17 mmol) was sealed inside a 11 mm i.d. × 20 cm evacuated Pyrex ampule. The sample was heated in a muffle furnace at a rate of 5 °C/min to 300 °C and held for 42 h. The dark brown residue was washed for 1 h in a 1:1 mixture of $CHCl_3$ and THF. The filtered product was dried overnight in a 60 °C vacuum oven. Yield: 59%. Elemental analysis calculated (%) for $C_{33}H_{20}$: C 95.81, H 4.19. Found: C 92.62, H 4.15.

Synthesis of "Click" Network 7. Tetrakis(4-azidophenyl)-methane (50 mg, 0.1 mmol), tetrakis(4-ethynyl)methane (42 mg, 0.1 mmol), sodium ascorbate (4 mg, 20 mol %), and copper sulfate (3 mg, 10 mol %) were added to a Radleyss reaction tube. The tube was sealed and evacuated and backfilled with N_2 gas five times. Thoroughly degassed, anhydrous THF (5 mL) was added to the reaction tube via syringe. Dry, degassed triethylamine (0.5 mL) was added via syringe. The reaction tube was slowly heated to 60 °C and maintained for 86 h. The reaction was carried out behind a blast screen. Once cooled to room temperature, 15 mL of methanol was added to the flask, and the precipitate was filtered and washed with H_2O, THF, acetone, and finally ether. The material was crushed and dried in air to yield an orange-brown powder. Yield: >100%. Elemental analysis calculated (%) for $C_{29}H_{18}N_6$: C 77.32, H 4.03, N 18.65. Found: C 65.69, H 4.50, N 14.58. **Safety note:** The thermal stability of tetrakis(4-azidophenyl)methane was tested before the reaction by differential scanning calorimetry (TA Instruments DSC Q2000). The onset of decomposition was observed to occur at 138 °C (see Supporting Information, Figure S4). The reaction was carried out on a small scale well below this temperature.

Gas Sorption Analysis. Polymer surface areas were initially screened using a Quantachrome NOVA 4200e surface area and pore size analyzer with a 5-point BET measurement between the pressure range of 0.05−0.25 P/P_0. Polymer surface areas and pore size distributions were measured by nitrogen adsorption and desorption at 77.3 K using either a Micromeritics ASAP 2420 or ASAP 2020 volumetric adsorption analyzer. The surface areas were calculated in the relative pressure (P/P_0) range from 0.01 to 0.1. Pore size distributions and pore volumes were derived from the adsorption branches of the isotherms using the nonlocal density functional theory (NL-DFT) pore model for pillared clay with cylindrical pore geometry. Samples were degassed at 300 °C for 18 h under vacuum (10^{-5} bar) before analysis. Hydrogen isotherms were measured at 77.3 K up to 1.12 bar using a Micromeritics ASAP 2420 volumetric adsorption analyzer.

Infrared Spectroscopy. FTIR spectra were collected on KBr disks in transmission mode using a Bruker Tensor 27. All spectra were measured with 16 scans at a resolution of 4 cm^{-1} using a blank KBr disk as background, followed by baseline correction.

Thermogravimetric Analysis (TGA). TGA analysis was carried out using a Q5000IR analyzer (TA Instruments) with an automated vertical overhead thermobalance. The samples were heated at the rate of 20 °C/min under a nitrogen atmosphere up to 1000 °C.

Powder X-ray Diffraction (PXRD). Powder X-ray diffraction data were collected on a Panalytical X'pert pro multipurpose diffractometer (MPD). Samples were mounted on a high-throughput Al plate and measured in transmission mode using Cu Kα radiation with a 2θ range of 5°−30°.

Results and Discussion

Synthesis. The general synthetic routes for the tetrahedral polymer networks are shown in Figures 1 and 2. These routes include Yamamoto coupling, Sonogashira−Hagihara cross-coupling, and palladium-catalyzed homocoupling. Yamamoto polymerization has recently been shown to be an efficient method to form porous polymer networks.[32,33] Similar methods were used here to synthesize networks **1**−**3** from the tetrahedral monomers tetrakis(4-iodophenyl)methane (TIPM), tetrakis(4-bromophenyl)silane (TBPS), and tetrakis(4-bromophenyl)-1,3,5,7-adamantane (TBPA), respectively. We demonstrated previously that Sonogashira−Hagihara palladium-catalyzed cross-coupling reactions can be used to synthesize microporous PAEs.[20−22,41] This methodology was used to cross-couple TIPM with tetrakis(4-ethynylphenyl)methane

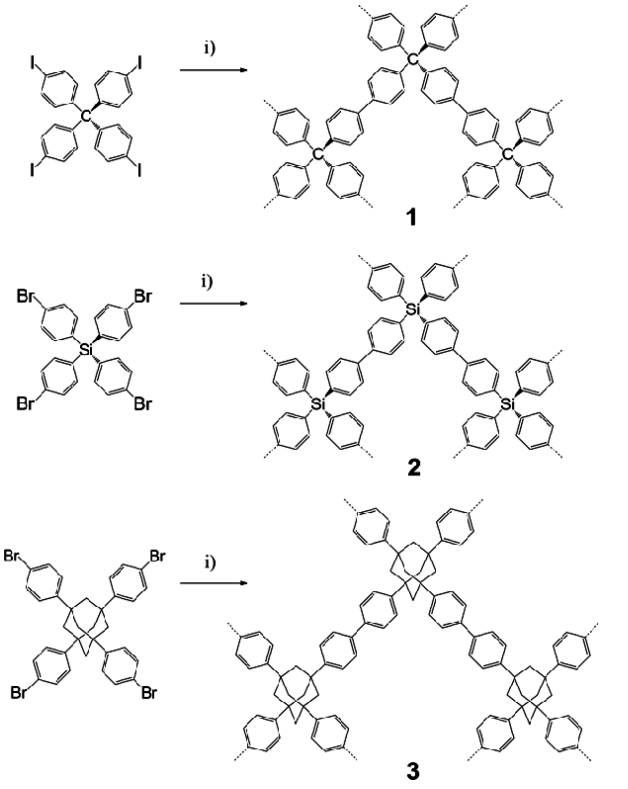

Figure 1. Synthetic route to polymer networks **1**−**3**. Conditions: (i) DMF, bis(1,5-cyclooctadiene)nickel(0), 2,2′-bipyridyl, 1,5-cyclooctadiene, 80 °C, 24 h.

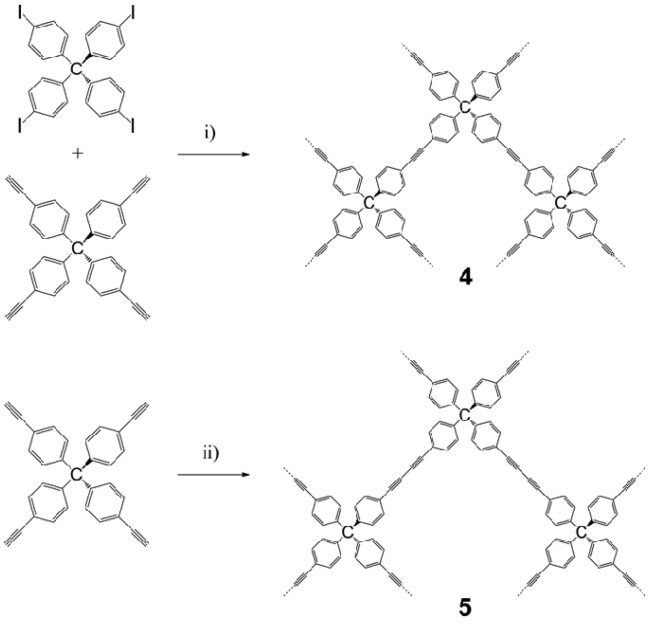

Figure 2. Synthetic routes to polymer networks **4** and **5**. Conditions: (i) DMF:diisopropylamine (1:1), $Pd(PPh_3)_4$, CuI, 80 C, 24 h; (ii) DMF: diisopropylamine (3:1), $PdCl_2(PPh_3)_2$, CuI, PPh_3, 70 °C, 86 h.

(TEPM) to form network **4**. We also showed previously that palladium-catalyzed chemistry can be employed for alkyne−alkyne homocoupling to produce porous poly(phenylene-butadiynes) (PPBs).[25] Other researchers extended this recently to prepare materials which adsorb large quantities of dihydrogen.[42] Some slight modifications were incorporated in the homocoupling of tetrakis(4-ethynylphenylmethane) in order to synthesize polymer network **5**. We used a method developed by Fairlamb and co-workers,[43] whereby additional triphenylphosphine ligand is added to the reaction to prevent byproduct formation. It was previously shown that a significant amount of cross-linking had occurred during the homocoupling, and evidence suggested the formation of head-to-tail 1,3-disubstituted enyenes.[25] DMF was employed as the solvent of choice, rather than toluene, since recent evidence suggests that this polar aprotic solvent yields higher surface areas in a range of CMP networks.[41]

As with the previously reported CMP networks,[20−22,25,36] the tan or orange-brown networks **4** and **5** precipitated from solution during the course of the reaction. Networks **1**−**3** precipitated as off-white powders. All networks were insoluble in all common organic solvents and required extensive washing and Soxhlet extraction in order to aid the removal of residual monomers and catalyst residues. TIPM, in particular, exhibits low solubility and requires extra care in its removal. Despite exhaustive washing, some of the polymer networks (**3** and **4**) still exhibit isolated yields in excess of 100%. This implies a degree of condensation which is lower than idealized levels and that terminal aryl halide and alkyne end groups might contribute to the sample mass, in addition to (potentially) residual unextracted catalysts. The synthesis of network **4** employs a 1.5 molar excess of TEPM, and any homocoupling[20−22,25,44] would also lead to higher-than-expected yields for the materials. By using the elemental analysis data in tandem with thermogravimetric analysis (TGA), the composition of networks **1**−**5** was explored further. Elemental analysis data is given in Table S1. The thermal combustion of the materials in air can lead to a measurement of the residual catalysts within the synthesized networks (see Figure S1 in the Supporting Information). Networks **1** and **3** showed < 0.5 wt % residue at 800 °C, while networks **4** and **5** showed residues of ∼3.2 wt %, indicating significant residual oxidized catalyst (PdO/CuO) in the materials, since any residual halides would be cleaved during combustion.[45] The Si-containing network **2** showed a residue of 17.8 wt %; assuming the formation of SiO_2 during combustion, the calculated amount of Si in the network would be 8.31 wt % (8.4 wt % theoretical). In the elemental analysis of networks **1**−**5**, the carbon contents were lower than predicted by theory, while hydrogen contents were higher; this has been observed for other CMP networks.[20−22,25] There was also a significant amount of residue in the elemental analysis. After accounting for the residues from the TGA data, all networks were found to contain approximately 3−4 wt % of unaccounted material. This difference can be rationalized by a combination of factors, in particular the presence of physisorbed water in the networks sequestered from the atmosphere postvacuum drying and also unreacted aryl halide end groups in the networks. It was noted that these materials appeared to moisten upon removal from the drying oven, suggesting a hygroscopic nature, which might explain the increased H content and decreased C content. This was also suggested recently as a possible reason for elemental analysis discrepancies by Liu et al.[30] Any further discrepancies might be accounted for by unreacted aryl halide groups, except for network **5** which should not have any residual halogen within the structure.

Structural Characterization. FTIR spectroscopy proved useful in probing the structure of networks **1**−**5**. The samples were pressed into KBr pellets for the spectral measurements. The KBr itself contains trace amounts of H_2O, as manifested in the spectra as broad peaks at 3400 and 1600 cm^{-1}. The samples themselves also contain physisorbed water in the

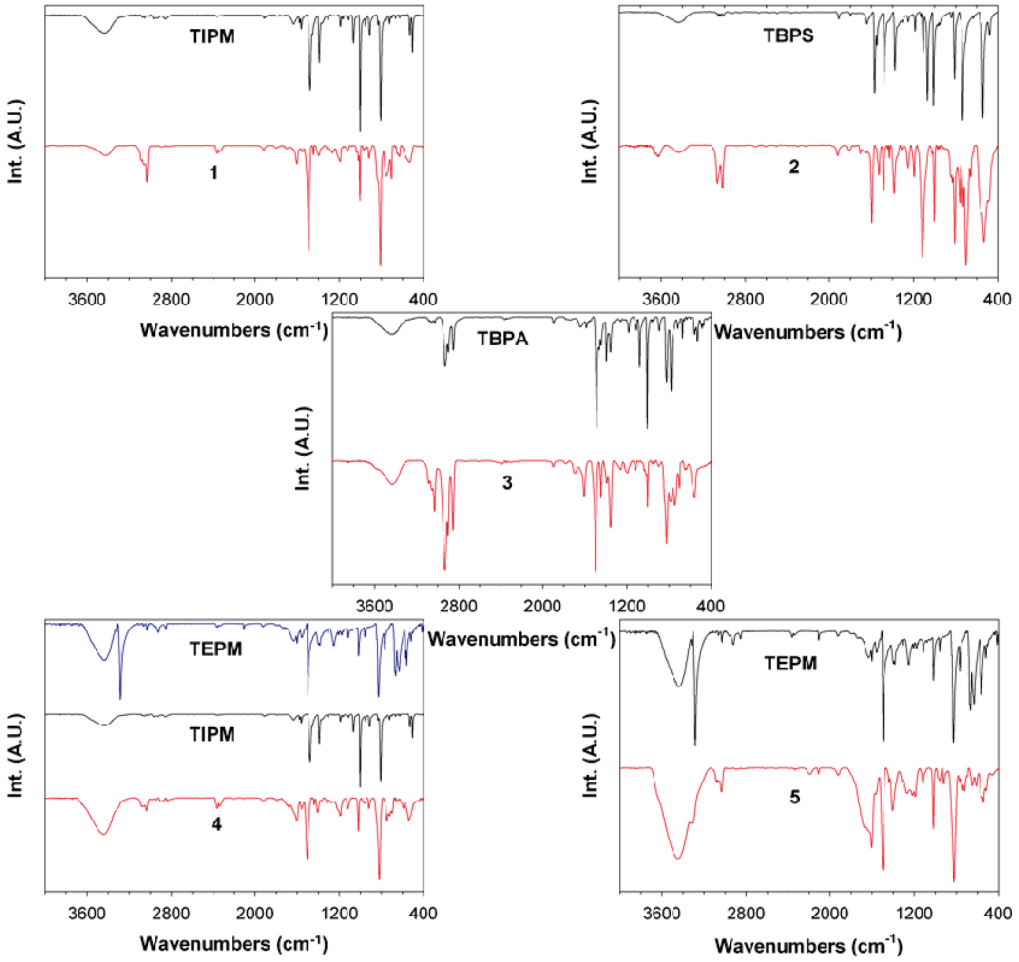

Figure 3. FTIR spectra for polymer networks **1**−**5** and respective starting materials, TIPM, TBPS, TBPA, and TEPM.

pore structure, as suggested by elemental analysis. This might be expected given their high surface areas. The Yamamoto polymers (**1**−**3**) were expected to show relatively little difference from their respective monomers in their IR spectra since the only change is the loss of the C−X stretching frequency. Comparison with FTIR spectra for the starting materials of TIPM, TBPS, and TBPA confirmed this: the only difference in the spectra for the networks was the disappearance of a single peak in the IR spectrum. Thomas and co-workers cited a peak at 1060 cm^{-1} as a C−Br oscillation in their study for a spirobifluorene-based network.[32] This same absorbance is observed in TIPM, TBPS, and TBPA and completely disappears in the spectra of the network products.

Other peaks in the spectrum are consistent with the anticipated network structures. For example, network **2** retains an intense peak near 1100 cm^{-1}, which has found to be a contribution from the Si−Ph bond.[46,47] There are also some low-intensity peaks near 3600, 1050, and 840 cm^{-1}, which suggests the presence of silanol (Si−OH) groups within the structure.[48] Network **3** exhibits the strong alkyl C−H peaks which correspond to the presence of the adamantane cage at the core of the monomer. Network **4** is the result of a cross-coupling between TIPM and TEPM; as such, the absorbance at 1060 cm^{-1} in TIPM should disappear, as should the C−H stretches from the terminal alkyne groups. This is observed in the IR spectrum of the product. A peak with very low intensity is also observed near 2111 cm^{-1} corresponding to the alkyne −C≡C− stretch. This would be expected to show low intensity given the symmetric nature of the alkyne. Network **5** is synthesized via homocoupling of alkyne groups

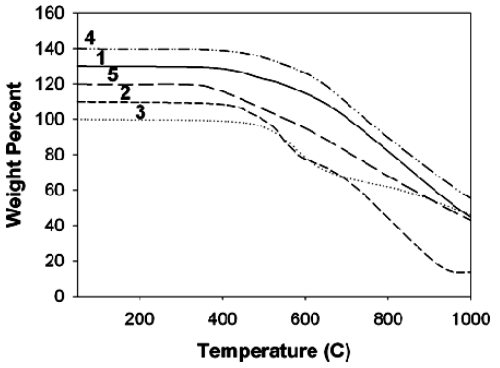

Figure 4. TGA thermograms for polymer networks **1**−**5**. The traces are offset by 10 units for the purposes of clarity.

to form butadiyne links between tetrahedral cores. The main observation should therefore be the disappearance of the intense alkynyl C−H stretch near 3300 cm^{-1}. This is greatly decreased in **5**, and a C≡C stretch is observed at 2111 cm^{-1}. Several peaks also appear near 3030 cm^{-1} which are not present in the starting material. This suggests the possible presence of alkenyl C−H groups within the network. Fairlamb made similar observations for reactions carried out at temperatures greater than 60 °C.[43] It appears therefore that at higher temperatures the triphenylphosphine ligand may not fully suppress extraneous cross-linking between alkyne groups.

The polymer networks were also characterized by powder X-ray diffraction (PXRD) (Figure S2 in Supporting Information)

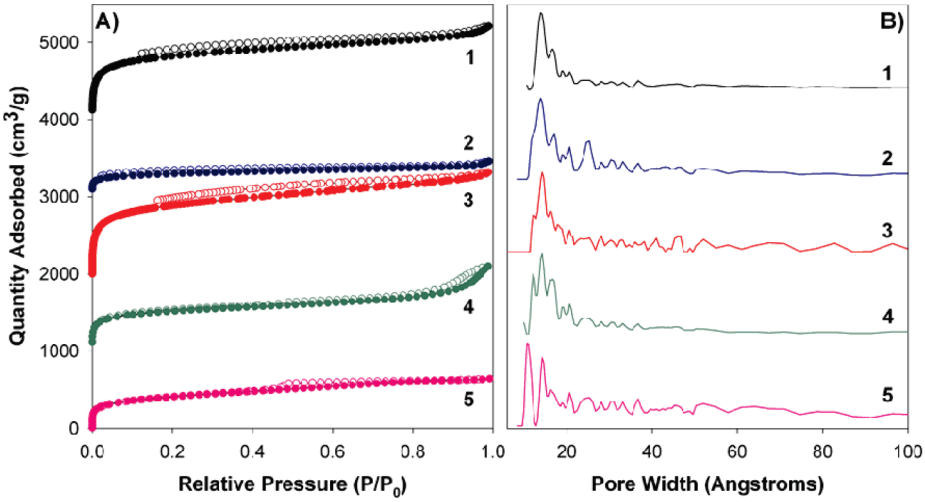

Figure 5. (A) Nitrogen adsorption/desorption isotherms (filled symbols = sorption; open symbols = desorption) and (B) pore size distribution curves for networks **1**−**5**, as calculated by NL-DFT. The isotherms in (A) have been offset by 1000 units for the purpose of clarity.

Table 1. Surface Properties and Gas Uptake for Networks 1−5

polymer network	SA_{BET} [m^2/g][a]	SA_{MICRO} [m^2/g][b]	V_{MICRO} [cm^3/g][c]	V_{TOTAL} [cm^3/g][d]	V_{MICRO}/V_{TOTAL}	H_2 uptake [wt %][e]	CO_2 uptake [wt %]
1	3160 ± 10	1867	0.98	1.54	0.64	2.13	6.54[f]
2	1102 ± 5	663	0.36	0.56	0.64	1.00	4.01[f]
3	3180 ± 20	1422	1.02	1.69	0.60	2.34	7.59[f]
4	1917 ± 5	888	0.53	0.94	0.56	1.67	6.63[g]
5	1470 ± 10	206	0.30	0.91	0.33	1.00	5.56[g]

[a] Surface area calculated from the N_2 adsorption isotherm using the BET method. [b] Micropore surface area calculated from the N_2 adsorption isotherm using *t*-plot method. [c] The micropore volume derived using the *t*-plot method based on the Halsey thickness equation. [d] Total pore volume at $P/P_0 = 0.99$. [e] Data were obtained by volumetric measurement at 77.3 K and 1.13 bar. [f] Data were obtained by volumetric measurement at 298 K and 1.13 bar. [g] Data were obtained by volumetric measurement at 298 K and 1.01 bar.

and thermogravimetric analysis (TGA) (Figure 4). Previous work within our group has shown no crystallinity whatsoever within CMP materials. The data shown in Figure S2 are provided as a comparison to data in the literature for PAF-1 where some limited evidence for crystallinity was reported based on broad peaks in the 5°−25° 2θ region.[33] By contrast, we observe no crystallinity for these samples. Networks **1**−**4** were found to possess good thermal stability and high decomposition temperatures of more than 500 °C in a nitrogen atmosphere. This is comparable with PAF-1 which showed thermal stability of up to 520 °C.[33] Network **5** demonstrated a somewhat lower decomposition temperature of ∼350 °C, which is consistent with previously reported homocoupled CMP networks.[25] All networks are more thermally stable than their starting materials (Supporting Information). TIPM, TBPS, TBPA, and TEPM show decomposition temperatures of 388, 343, 418, and 214 °C, respectively. TEPM is interesting because the starting material begins to decompose at 220 °C and loses ∼5 wt % and then maintains that weight until 400 °C. It has been previously reported that terminal alkynes can polymerize via several different pathways at high temperatures to form polymeric structures.[49−52] These pathways include cyclotrimerization, biradical mechanisms which yield naphthalenic connections, Glaser coupling (diyne formation), and Straus coupling (enyne formation).[49,50] As a proof of concept, we heated a sample of solid TEPM inside a vacuum-sealed ampule at 300 °C whereupon a dark brown polymer, **6**, was produced. FTIR spectra of this insoluble material demonstrated loss of the alkyne C−H stretch at 3300 cm^{-1}, and the network demonstrated a modest BET surface area of 625 m^2/g (see Supporting Information).

Gas Sorption Analysis. The porosity in the networks was investigated by sorption analysis using N_2, CO_2, and H_2 as the sorbate molecules. Figure 5A shows the N_2 adsorption and desorption isotherms for polymers **1**−**5**, while Table 1 summarizes the porous properties of each network. Networks **1**, **2**, **3**, and **5** gave rise to type I isotherms, while network **4** displayed a type I isotherm with type IV character at higher relative pressures. All of the desorption isotherms for the five networks exhibit hysteresis to a degree, suggesting the presence of some mesopores (2−50 nm) within the materials.

Figure 5B shows the pore size distribution (PSD) curves for the three polymer networks as calculated using nonlocal density functional theory (NL-DFT). Networks **1**−**4** exhibited micropore diameters centering around 1.4 with a shoulder peak in the 1.6−1.7 nm region. Additionally, **2**−**4** showed a second shoulder at 1.1 nm. Network **5** showed a major distribution near 1.1 nm while a second distribution was centered around 1.4 nm. All of the networks showed weak peaks in the size range 2−5 nm while **3** and **5** showed more peaks in the 6−10 nm region. The PSD curves agree with the shape of the N_2 isotherms (Figure 5A) and suggest that the structures all feature mesopores within the structures as well as micropores. The contribution of microporosity to the networks can be calculated as the ratio of the micropore volume, V_{MICRO}, over the total pore volume, V_{TOTAL}. The ratios indicate networks **1**−**4** possess a ratio of 0.64, 0.64, 0.60, and 0.56, respectively. Network **5** ($V_{MICRO}/V_{TOTAL} = 0.33$) possesses a more significant contribution from mesopores. Networks **1** and **3** demonstrate the highest surface areas (3168 and 3177 m^2/g, respectively) among the five polymer networks. These materials exceed the surface areas of most other microporous organic polymers with the exception of

PAF-1[33] and a carbonized CTF.[9,33] PAF-1, which is isostructural to **1**, demonstrated a surface area of 5600 m^2/g. Network **4** is notable since it is the most porous PAE network prepared so far (SA_{BET} = 1917 m^2/g).[20−22,25,27,41,44] Network **4** also has significantly higher surface area than the recently reported isostructural CMP material synthesized from TIPM and acetylene gas.[53]

The permanent porosity in these networks results from the highly cross-linked, rigid structure and the presence of tetrahedral nodes. Presumably, the most porous materials are unable to interpenetrate effectively and fill space, thus leading to the formation of accessible pores and high surface areas. It has been demonstrated for CMP networks that the length of the strut between the connecting nodes affects the average pore size obtained.[20−22] In particular, it was suggested that the increased degree of conformational freedom in the longer struts allows for greater intermolecular and intramolecular intercalation and more efficient space filling in the structures. This contributes to the decreased micropore volume and lower surface areas observed for networks with longer struts.[20−22] In this study, the micropore volume is strongly correlated to the surface area (Table 1), but there is no simple relationship between strut length and surface area. In this series of polymers, the ranking of strut lengths (estimated from simple geometric calculations) from largest to smallest would be **5** > **3** > **4** > **2** > **1**. By analogy with other studies,[20−22] **5** might therefore be predicted to possess the lowest surface area while **1** should have the highest. In fact, network **3** possesses the highest surface area and networks **4** and **2** show significantly lower surface areas. This lack of a simple strut length relationship might result from the more diverse linking chemistry used in this study since other "strut length" studies of this kind involved just one coupling chemistry to create homologous series of networks.[20−22] It is likely therefore that the efficiency of the network condensation reaction has a profound effect on the resulting materials properties. Network **1**, for example, was synthesized from TIPM: aryl bromides, not iodides, are usually employed in Yamamoto coupling reactions, and it is possible that reaction efficacy is reduced for TIPM. For example, Swager et al. reported on the homopolymerization of 2,6-halotriptycenes and found the iodo monomer produced much lower molecular weight polymers when compared with the bromo derivative.[54] This might also explain the somewhat lower surface area observed in **1** in comparison to PAF-1.[33] Silane-based **2** should possess strut lengths which are very similar to those in **1**, and in this case the tetrabrominated monomer, TBPS, was employed. There are indications from the FTIR spectrum that a side reaction is occurring in this case. We have previously used TBPS in the synthesis of CMP networks and solid state NMR evidence suggests that a proportion of the central Si−C bonds were hydrolyzed during network formation.[36] Analogous side reactions might occur during the formation of **2** which could lead to structural defects and subsequent surface area reduction. Structural defects seem quite likely in the case of networks **4** and **5**. As discussed above, the elemental analysis of **4** and **5** suggest significant amounts of unreacted end groups. It is possible that the reaction efficiency of Sonogashira−Hagihara coupling chemistry is inherently less favorable for the formation of ultrahigh surface area microporous organic polymers with respect to Yamamoto routes or, alternatively, that alternative preparation methods need to be considered.

The need for coupling chemistry with high reaction conversions led us to consider to "click" chemistry.[55−57] Despite the large amount of literature in this area, there are few examples of conjugated polymers synthesized by "click" routes.[58−60]

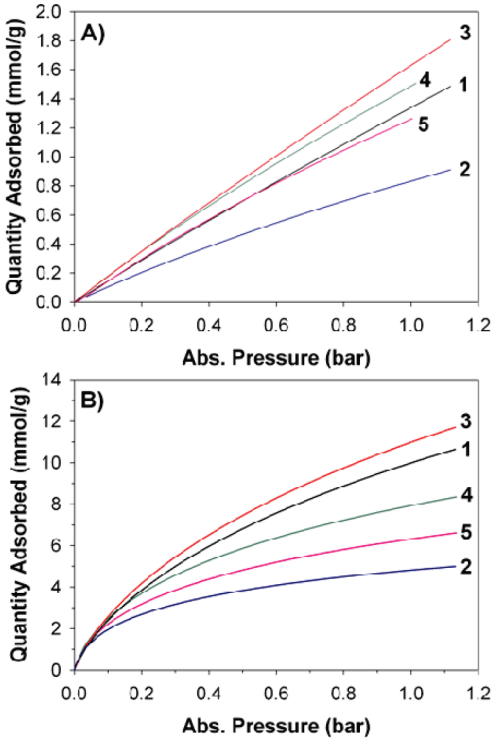

Figure 6. Gas uptake data for networks **1**−**5**: (A) CO_2 isotherms measured at 298 K and (B) H_2 isotherms measured at 77.3 K.

There are no previous examples of the use of click chemistry to synthesize porous organic polymers. We therefore synthesized the corresponding tetrahedral-based polytriazole from TEPM and tetrakis(4-azidophenyl)methane (TAzPM).[40] Adapting a method employed by Jin and co-workers,[60] network **7** was synthesized as an orange-brown powder. TGA analysis (Supporting Information) indicated a substantial quantity of H_2O being removed from this sample at temperatures up to 60 °C, despite the sample being degassed beforehand at 100 °C. The analysis also indicates a mass loss of ~3.2 wt.% between 125 and 275 °C, suggesting perhaps that residual azide and alkyne end groups were decomposing. The FTIR spectrum of **7** (Supporting Information) indicates the presence of physisorbed H_2O and azide/alkyne groups near 2100 cm^{-1}. The alkynyl C≡C−H stretch at 3300 cm^{-1} is absent from the polymer spectrum, and azide intensity is greatly diminished when compared to the starting material, suggesting the formation of 1,2,3-triazole linking units. A BET surface area of 1128 m^2/g was measured for this "clicked" CMP network.

The H_2 and CO_2 sorption properties of the polymers were investigated by volumetric methods at 77.3 and 298 K, respectively. Figure 6 shows the CO_2 and H_2 adsorption isotherms up to a maximum H_2 pressure of 1.13 bar. Network **3** exhibits the highest CO_2 uptake (1.81 mmol/g/7.59 wt % at 1.13 bar); in fact, it is higher than that reported for PAF-1,[33] despite having a lower surface area. Additionally, it was found that network **4** exhibits a higher CO_2 adsorption capacity than **1** even though its apparent BET surface area is lower. Even **5**, which exhibits approximately half of the surface area of network **1**, produced comparable CO_2 uptake. It is possible that the alkyne groups present within the linker offer favorable interactions with the sorbate compared with those containing only phenyl-based linkers. Alternatively, this difference may arise from pore size distribution effects. The H_2 uptake sorption properties of networks **1**−**5** can be correlated directly with the micropore surface area

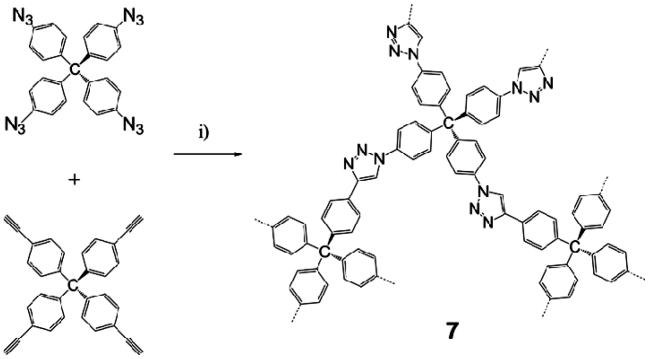

Figure 7. Synthetic route for network **6**. Conditions: (i) THF:triethylamine (10:1), 10 mol % $CuSO_4$, 20 mol % sodium ascorbate, 60 °C, 84 h.

and micropore volume. The networks with the highest micropore surface areas and micropore volumes (Table 1) gave rise to the highest uptakes at low pressures because micropores, not mesopores, contribute mainly to H_2 adsorption at these pressures and temperatures. Network **3** exhibits the largest H_2 uptake of 11.71 mmol/g at 1.13 bar/77.3 K (2.34 wt %), somewhat higher than values reported recently for triptycene-based PIMs.[61] In terms of volumetric capacity, network **3** demonstrated a density of 1.15(2) g/cm^3; this equates to a hydrogen volumetric capacity of 0.027 kg H_2/L. This is below the U.S. Department of Energy's 2015 targets for onboard hydrogen storage systems for light-duty vehicles, which is 0.040 kg H_2/L and well below the ultimate target of 0.070 kg H_2/L.[62]

Conclusions

We have synthesized a series of conjugated microporous polymer networks by using Yamamoto coupling or Sonogashira−Hagihara cross-coupling chemistries from a variety of tetrahedral-shaped monomers. The thermally stable polymers exhibit very surface areas (up to 3200 m^2/g) and adsorb up to 2.34 wt.% hydrogen by mass at 1.13 bar/77 K. The networks have higher surface areas than most other amorphous organic polymers, with only PAF-1 exhibiting a higher SA_{BET} value.[33] These results reinforce the benefits of tetrahedral monomers for the generation of high surface area materials. The study suggests that the efficacy of the chemistry and the monomer reactivity have a pronounced effect on the surface areas attained in addition to the monomer structure and network strut length. Broadly speaking, the Yamamoto polymerization appears to produce fewer residual end groups in the synthesis of microporous organic polymers when compared to Sonogashira−Hagihara chemistry. In general, higher levels of condensation might be expected to lead to less interpenetration and a greater degree of permanent pore volume. A preliminary attempt to employ "click" chemistry led to a porous network comprised of triazole linkages, suggesting that this too may be a viable chemistry platform for producing high nitrogen-content microporous solids, although there are safety issues to be considered in terms of scaling such routes. Future studies will focus on functionalization of such networks and their use in applications such as gas capture.

Acknowledgment. We thank the EPSRC (EP/C511794/1 and EP/P503914/1) for financial support. A.I.C. is a Royal Society Wolfson Merit Award holder.

Supporting Information Available: Powder X-ray diffraction patterns of starting materials TEPM, TBPS, TBPA, TIPM, and polymer networks **1**−**5**; TGA thermograms and FTIR spectra for polymer networks **6** and **7** as well as starting materials; differential scanning calorimetry (DSC) plot for TAzPM; and 5-point BET adsorption measurements of **6** and **7**. This material is available free of charge via the Internet at http://pubs.acs.org.

References and Notes

(1) McKeown, N. B.; Budd, P. M. *Chem. Soc. Rev.* **2006**, *35*, 675.
(2) Morris, R. E.; Wheatley, P. S. *Angew. Chem., Int. Ed.* **2008**, *47*, 4966.
(3) Mackintosh, H. J.; Budd, P. M.; McKeown, N. B. *J. Mater. Chem.* **2008**, *18*, 573.
(4) Schmidt, J.; Weber, J.; Epping, J. D.; Antonietti, M.; Thomas, A. *Adv. Mater.* (*Weinheim, Ger.*) **2009**, *21*, 702.
(5) Cote, A. P.; Benin, A. I.; Ockwig, N. W.; O'Keeffe, M.; Matzger, A. J.; Yaghi, O. M. *Science* (*Washington, DC, United States*) **2005**, *310*, 1166.
(6) El-Kaderi, H. M.; Hunt, J. R.; Mendoza-Cortes, J. L.; Cote, A. P.; Taylor, R. E.; O'Keeffe, M.; Yaghi, O. M. *Science* (*Washington, DC, U. S.*) **2007**, *316*, 268.
(7) Uribe-Romo, F. J.; Hunt, J. R.; Furukawa, H.; Kloeck, C.; O'Keeffe, M.; Yaghi, O. M. *J. Am. Chem. Soc.* **2009**, *131*, 4570.
(8) Kuhn, P.; Antonietti, M.; Thomas, A. *Angew. Chem., Int. Ed.* **2008**, *47*, 3450.
(9) Kuhn, P.; Forget, A.; Su, D.; Thomas, A.; Antonietti, M. *J. Am. Chem. Soc.* **2008**, *130*, 13333.
(10) Tsyurupa, M. P.; Davankov, V. A. *React. Funct. Polym.* **2002**, *53*, 193.
(11) Ahn, J.-H.; Jang, J.-E.; Oh, C.-G.; Ihm, S.-K.; Cortez, J.; Sherrington, D. C. *Macromolecules* **2006**, *39*, 627.
(12) Lee, J. Y.; Wood, C. D.; Bradshaw, D.; Rosseinsky, M. J.; Cooper, A. I. *Chem. Commun.* **2006**, 2670.
(13) Wood, C. D.; Tan, B.; Trewin, A.; Niu, H.; Bradshaw, D.; Rosseinsky, M. J.; Khimyak, Y. Z.; Campbell, N. L.; Kirk, R.; Stoeckel, E.; Cooper, A. I. *Chem. Mater.* **2007**, *19*, 2034.
(14) McKeown, N. B.; Budd, P. M. *Macromolecules* **2010**, *43*, 5163.
(15) Budd, P. M.; Ghanem, B. S.; Makhseed, S.; McKeown, N. B.; Msayib, K. J.; Tattershall, C. E. *Chem. Commun.* (*Cambridge, U. K.*) **2004**, 230.
(16) McKeown, N. B.; Hanif, S.; Msayib, K.; Tattershall, C. E.; Budd, P. M. *Chem. Commun.* (*Cambridge, U. K.*) **2002**, 2782.
(17) McKeown, N. B.; Makhseed, S.; Budd, P. M. *Chem. Commun.* (*Cambridge, U. K.*) **2002**, 2780.
(18) Ghanem, B. S.; Hashem, M.; Harris, K. D. M.; Msayib, K. J.; Xu, M.; Budd, P. M.; Chaukura, N.; Book, D.; Tedds, S.; Walton, A.; McKeown, N. B. *Macromolecules* **2010**, *43*, 5287.
(19) Chinchilla, R.; Najera, C. *Chem. Rev.* (*Washington, DC, U. S.*) **2007**, *107*, 874.
(20) Jiang, J.-X.; Su, F.; Wood, C. D.; Campbell, N. L.; Niu, H.; Dickinson, C.; Ganin, A. Y.; Rosseinsky, M. J.; Khimyak, Y. Z.; Cooper, A. I.; Trewin, A. *Angew. Chem., Int. Ed.* **2007**, *46*, 8574.
(21) Jiang, J.-X.; Su, F.; Trewin, A.; Wood, C. D.; Niu, H.; Jones, J. T. A.; Khimyak, Y. Z.; Cooper, A. I. *J. Am. Chem. Soc.* **2008**, *130*, 7710.
(22) Jiang, J.-X.; Trewin, A.; Su, F.; Wood, C. D.; Niu, H.; Jones, J. T. A.; Khimyak, Y. Z.; Cooper, A. I. *Macromolecules* **2009**, *42*, 2658.
(23) Cooper, A. I. *Adv. Mater.* **2009**, *21*, 1291.
(24) Dawson, R.; Su, F.; Niu, H.; Wood, C. D.; Jones, J. T. A.; Khimyak, Y. Z.; Cooper, A. I. *Macromolecules* **2008**, *41*, 1591.
(25) Jiang, J.-X.; Su, F.; Niu, H.; Wood, C. D.; Campbell, N. L.; Khimyak, Y. Z.; Cooper, A. I. *Chem. Commun.* (*Cambridge, U. K.*) **2008**, 486.
(26) Chen, L.; Honsho, Y.; Seki, S.; Jiang, D. *J. Am. Chem. Soc.* **2010**, *132*, 6742.
(27) Weber, J.; Thomas, A. *J. Am. Chem. Soc.* **2008**, *130*, 6334.
(28) Xia, J.; Yuan, S.; Wang, Z.; Kirklin, S.; Dorney, B.; Liu, D.-J.; Yu, L. *Macromolecules* **2010**, *43*, 3325.
(29) Yuan, S.; Kirklin, S.; Dorney, B.; Liu, D.-J.; Yu, L. *Macromolecules* **2009**, *42*, 1554.
(30) Yuan, S.; Dorney, B.; White, D.; Kirklin, S.; Zapol, P.; Yu, L.; Liu, D.-J. *Chem. Commun.* (*Cambridge, U. K.*) **2010**, *46*, 4547.
(31) Sprick, R. S.; Thomas, A.; Scherf, U. *Polym. Chem.* **2010**, *1*, 283.
(32) Schmidt, J.; Werner, M.; Thomas, A. *Macromolecules* **2009**, *42*, 4426.
(33) Ben, T.; Ren, H.; Ma, S.; Cao, D.; Lan, J.; Jing, X.; Wang, W.; Xu, J.; Deng, F.; Simmons, J. M.; Qiu, S.; Zhu, G. *Angew. Chem., Int. Ed.* **2009**, *48*, 9457.
(34) Furukawa, H.; Ko, N.; Go, Y. B.; Aratani, N.; Choi, S. B.; Choi, E.; Yazaydin, A. O.; Snurr, R. Q.; O'Keeffe, M.; Kim, J.; Yaghi, O. M. *Science* **2010**, *329*, 424.

(35) Rose, M.; Boehlmann, W.; Sabo, M.; Kaskel, S. *Chem. Commun.* (*Cambridge, U. K.*) **2008**, 2462.
(36) Stöckel, E.; Wu, X.; Trewin, A.; Wood, C. D.; Clowes, R.; Campbell, N. L.; Jones, J. T. A.; Khimyak, Y. Z.; Adams, D. J.; Cooper, A. I. *Chem. Commun.* (*Cambridge, U. K.*) **2009**, 212.
(37) Su, D.; Menger, F. M. *Tetrahedron Lett.* **1997**, *38*, 1485.
(38) Rathore, R.; Burns, C. L.; Guzei, I. A. *J. Org. Chem.* **2004**, *69*, 1524.
(39) Liao, Y.; Baskett, M.; Lahti, P. M.; Palacio, F. *Chem. Commun.* (*Cambridge, U. K.*) **2002**, 252.
(40) Plietzsch, O.; Schilling, C. I.; Tolev, M.; Nieger, M.; Richert, C.; Muller, T.; Brase, S. *Org. Biomol. Chem.* **2009**, *7*, 4734.
(41) Dawson, R.; Laybourn, A.; Khimyak, Y. Z.; Adams, D. J.; Cooper, A. I. *Macromolecules* **2010**, DOI: 10.1021/ma101541h.
(42) Li, A.; Lu, R. F.; Wang, Y.; Wang, X.; Han, K. L.; Deng, W. Q. *Angew. Chem., Int. Ed.* **2010**, *49*, 3330.
(43) Fairlamb, I. J. S.; Baeuerlein, P. S.; Marrison, L. R.; Dickinson, J. M. *Chem. Commun.* (*Cambridge, U. K.*) **2003**, 632.
(44) Dawson, R.; Laybourn, A.; Clowes, R.; Khimyak, Y. Z.; Adams, D. J.; Cooper, A. I. *Macromolecules* **2009**, *42*, 8809.
(45) Roll, M. F.; Kampf, J. W.; Kim, Y.; Yi, E.; Laine, R. M. *J. Am. Chem. Soc.* **2010**, *132*, 10171.
(46) Henry, M. C.; Noltes, J. G. *J. Am. Chem. Soc.* **1960**, *82*, 555.
(47) Warner, S. D.; Butler, I. S.; Wharf, I. *Spectrochim. Acta, Part A* **2000**, *56*, 453.
(48) Bueno, W. A. *Spectrochim. Acta, Part A* **1980**, *36*, 1059.
(49) Swanson, S. A.; Fleming, W. W.; Hofer, D. C. *Macromolecules* **1992**, *25*, 582.
(50) Gandon, S.; Mison, P.; Bartholin, M.; Mercier, R.; Sillion, B.; Geneve, E.; Grenier, P.; Grenier-Loustalot, M. F. *Polymer* **1997**, *38*, 1439.
(51) Reichert, V. R.; Mathias, L. J. *Macromolecules* **1994**, *27*, 7030.
(52) Asuncion, M. Z.; Roll, M. F.; Laine, R. M. *Macromolecules* **2008**, *41*, 8047.
(53) Choi, J. H.; Choi, K. M.; Jeon, H. J.; Choi, Y. J.; Lee, Y.; Kang, J. K. *Macromolecules* **2010**, *43*, 5508.
(54) Chen, Z.; Swager, T. M. *Macromolecules* **2008**, *41*, 6880.
(55) Rostovtsev, V. V.; Green, L. G.; Fokin, V. V.; Sharpless, K. B. *Angew. Chem., Int. Ed.* **2002**, *41*, 2596.
(56) Meldal, M.; Tornøe, C. W. *Chem. Rev.* **2008**, *108*, 2952.
(57) Binder, W. H.; Sachsenhofer, R. *Macromol. Rapid Commun.* **2007**, *28*, 15.
(58) Steenis, D. J. V. C. v.; David, O. R. P.; Strijdonck, G. P. F. v.; Maarseveen, J. H. v.; Reek, J. N. H. *Chem. Commun.* **2005**, 4333.
(59) Bakbak, S.; Leech, P. J.; Carson, B. E.; Saxena, S.; King, W. P.; Bunz, U. H. F. *Macromolecules* **2006**, *39*, 6793.
(60) Karim, M. A.; Cho, Y.-R.; Park, J. S.; Ryu, T. I.; Lee, M. J.; Song, M.; Jin, S.-H.; Lee, J. W.; Gal, Y.-S. *Macromol. Chem. Phys.* **2008**, *209*, 1967.
(61) Ghanem, B. S.; Hashem, M.; Harris, K. D. M.; Msayib, K. J.; Xu, M.; Budd, P. M.; Chaukura, N.; Book, D.; Tedds, S.; Walton, A.; McKeown, N. B. *Macromolecules* **2010**.
(62) Talipov, S. A.; Tadjimukhamedov, F. K.; Hulliger, J.; Ibragimov, B. T.; Yuldashev, A. *Cryst. Eng.* **2003**, *6*, 137.